

# Effects of strain rate on entropy generation in laminar counterflow diffusion flames

Silu Xue, Wang Han, Lijun Yang

School of Astronautics, Beihang University, Beijing 100191, China

## 1 Introduction

Understanding combustion-generated noise helps to control thermoacoustic instabilities encountered in rocket and gas-turbine engines. It is well known that there are two types of combustion noise, i.e., direct combustion noise and indirect combustion noise [1]. The direct combustion noise is a monopole sound source associated with the unsteady expansion/compression of burned gases. On the other hand, the indirect combustion noise is a dipole sound source, which is generated by accelerating the entropy fluctuations through a nozzle leads to acoustic fluctuations, due to the fluctuations in fluid density caused by the unsteady force associated with acceleration [2]. It is noted that the indirect combustion noise is an important noise source in the combustor [1].

Given that entropy generation is of importance for the indirect combustion noise, significant progresses on the investigations of entropy generation in flames have been made in the literature. In general, there are two pathways for entropy generation in reaction systems, namely molecular transport, and chemical reaction, in which exothermic reactions generate entropy by a variety of mechanisms, including heat release, the change in number of moles of species, and the change in species. The spatial dependence of the different sources of entropy generation was investigated by Nishida et al. [3] in premixed hydrogen flames, and their results indicate that the chemical reaction terms are the dominant source of entropy generation with a non-negligible contribution from molecular diffusion effects. Liu et al. [4] investigated and compared the entropy production and exergy loss characteristics at engine relevant conditions. Their results indicate that compared to chemical reactions, the entropy production and exergy destruction due to heat and species mass transfer is negligible when autoignition mode is dominant over flame propagation in premixed flames.

Recently, Patki et al. [5] examined the mechanisms of entropy production due to exothermic chemical reactions in laminar, premixed flames. They decomposed the chemical source term into three sub-terms by introducing the sensible enthalpy term and partial entropy term:

$$S_e = S_{e,1} + S_{e,2} + S_{e,3} = \dot{q} - \sum_{i=1}^N \dot{\omega}_i \int_{T_0}^T c_{p,i} dT + \sum_{i=1}^N T S_i \dot{\omega}_i \quad (1)$$

where  $S_{e,1}$  denotes the unsteady heat release rate,  $S_{e,2}$  and  $S_{e,3}$  represent the sensible enthalpy term and the partial entropy term, respectively.  $S_{e,3}$  is difficult to analyze because it consists of the sum of the entropy of reactants and products in comparable magnitudes and opposite signs. In addition,  $S_{e,3}$  is

strongly influenced by dissociation, which reduces the quantity of major species and increases minor species into the products. In other words, the sign of  $S_{e,3}$  term cannot be estimated by analyzing major species alone. For oxy-fueled systems, Patki et al. [5] introduced  $S_{e,3,major}$ , which is defined as the contribution to  $S_{e,3}$  from four major species: fuel,  $O_2$ ,  $CO_2$ ,  $H_2O$ :

$$S_{e,3,major} = TS_{fuel}\dot{\omega}_{fuel} + TS_{O_2}\dot{\omega}_{O_2} + TS_{CO_2}\dot{\omega}_{CO_2} + TS_{H_2O}\dot{\omega}_{H_2O} \quad (2)$$

It was found that the unsteady, exothermic heat release, i.e.  $S_{e,1}$ , is the dominant term in air breathing systems, but the combined influence of the other terms,  $S_{e,2}$  and  $S_{e,3}$  (i.e. the sensible enthalpy term and the partial entropy term), can outweigh  $S_{e,1}$  in oxy-fueled systems.

It is noted that Patki et al. [5] only investigated the entropy production in freely premixed propagation flames, which leads to the effect of strain rate being not taken into account. Moreover, there are only a few studies on the entropy generation in diffusion flame. In this context, the objective of this work is to investigate the entropy production mechanism of (strained) counterflow diffusion flames at different pressures conditions.

## 2 Numerical Methods

In this work, one-dimensional counterflow diffusion flames are simulated using Cantera [6]. As shown in Fig. 1, the oxidizer stream is pure oxygen with a uniform velocity of  $U_O$ , and the fuel stream (methane or hydrogen here) is supplied from the bottom with a uniform velocity of  $U_F$ . The distance between the two nozzles is 2 cm, and the inlet temperature is 300 K for both. The ratio of fuel inlet velocity to that of the oxidizer is determined based on the momentum balance,  $U_F/U_O = \sqrt{\rho_O/\rho_F}$ , where  $\rho_O$  and  $\rho_F$  are densities of the mixtures in the oxidizer and fuel stream, respectively. The configuration is characterized by the global strain rate:

$$a = \frac{2U_O}{L} \left( 1 + \frac{U_F\sqrt{\rho_F}}{U_O\sqrt{\rho_O}} \right) = \frac{4U_O}{L} \quad (3)$$

GRI-Mech 3.0 [7] mechanism with 325 reactions and 53 species is used for methane-oxygen and hydrogen-oxygen flame calculations.

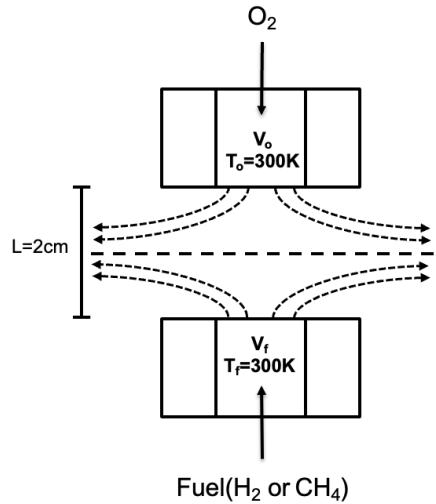


Figure 1: One-dimensional counterflow diffusion-flame configuration

### 3 Results and Discussion

From equation (3), it can be seen that by changing the speed of the oxidizer inflow  $U_O$ , different strain rates can be obtained. The strain rates considered in this work are shown in Table 1.

Table 1: Strain rates considered in this work.

$U_O/m/s$	0.25	0.85	1.45	2.05	2.65	3.25	3.85	4.45	5.05	5.65
$a/s^{-1}$	50	170	290	410	530	650	770	890	1010	1130

Similar to Patki et al. [5], the relative contributions of  $S_{e,1}$ ,  $S_{e,2}$  and  $S_{e,3}$  as well as their flame integration ratio will be discussed in the following. The flame integration ratio is defined as follows [5]:

$$\alpha_1 = \frac{\int S_{e,1} dx}{\int S_e dx}, \alpha_2 = \frac{\int S_{e,2} dx}{\int S_e dx}, \alpha_3 = \frac{\int S_{e,3} dx}{\int S_e dx}, \alpha_{3,major} = \frac{\int S_{e,3,major} dx}{\int S_e dx} \quad (4)$$

#### 3.1 Sources of entropy generation

Figures 2 and 3 plot the spatial profiles of the total source term, i.e.  $S_e$ , as well as  $S_{e,1}$ ,  $S_{e,2}$ , and  $S_{e,3}$  at six different strain rates and  $p = 1$  atm for counterflow diffusion  $CH_4/O_2$  and  $H_2/O_2$  flames, respectively. Figure 2 shows that  $S_{e,1}$  dominates over other terms, and that both  $S_{e,3}$  and  $S_{e,1}$  play a substantial role in entropy generation. Similarly, Fig. 3 shows that for the  $H_2/O_2$  case,  $S_{e,1}$  and  $S_{e,3}$  are dominant, and that the effect of  $S_{e,2}$  is small. Both Fig. 2 and Fig. 3 demonstrate that the contribution of  $S_e$ ,  $S_{e,1}$ ,  $S_{e,2}$  and  $S_{e,3}$  to entropy generation significantly increases with strain rate.

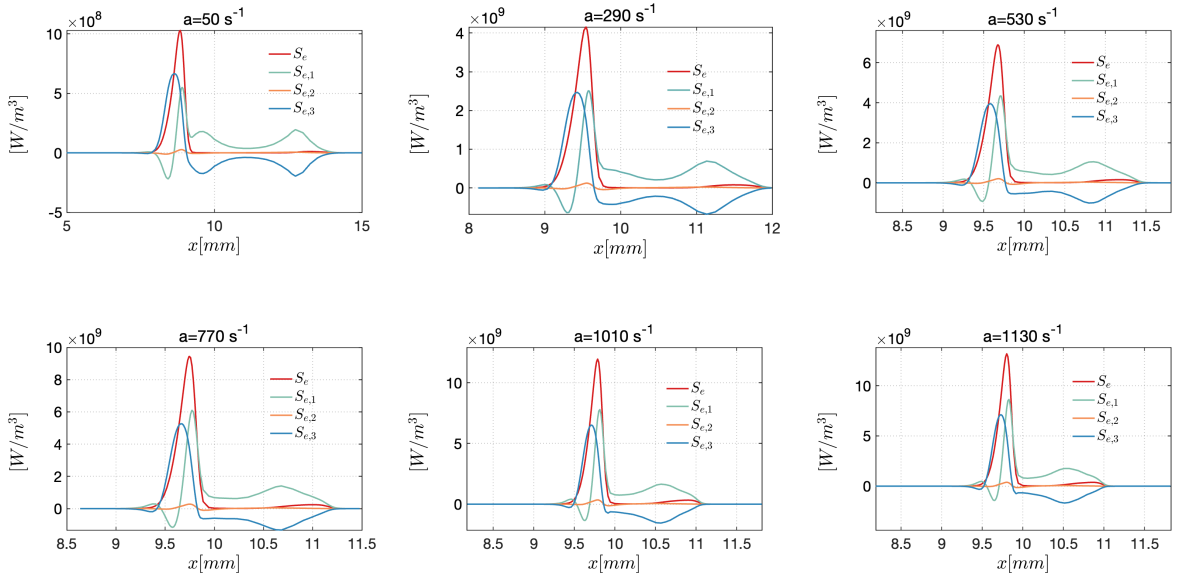


Figure 2: Spatial distributions of  $S_{e,1}$ ,  $S_{e,2}$ , and  $S_{e,3}$  for  $CH_4/O_2$  combustion at six different strain rates and  $p = 1$  atm.

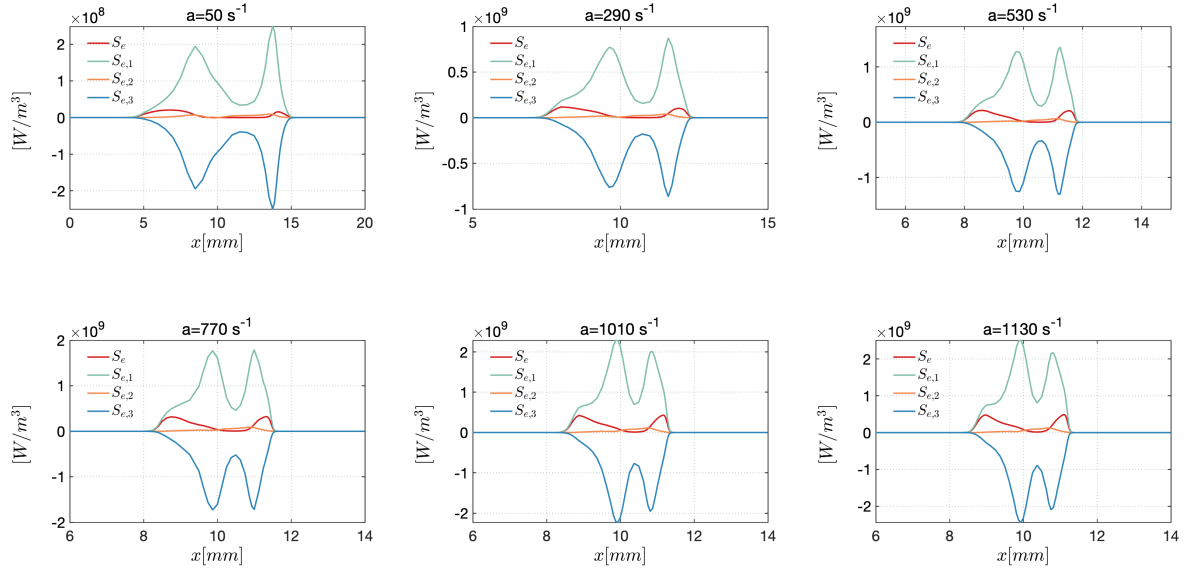


Figure 3: Spatial distributions of  $S_{e,1}$ ,  $S_{e,2}$  and  $S_{e,3}$  for  $H_2/O_2$  combustion at six different strain rates and  $p = 1$  atm.

Figure 4 compares  $S_{e,3}$  with  $S_{e,3,major}$  for  $CH_4/O_2$  and  $H_2/O_2$  flames at  $a = 530 s^{-1}$  and  $p = 1$  atm. It is seen that the model of  $S_{e,3}$  via  $S_{e,3,major}$  cannot accurately capture the contribution of  $S_{e,3}$ . This indicate that the minor species have a significant impact on the contribution of  $S_{e,3}$ .

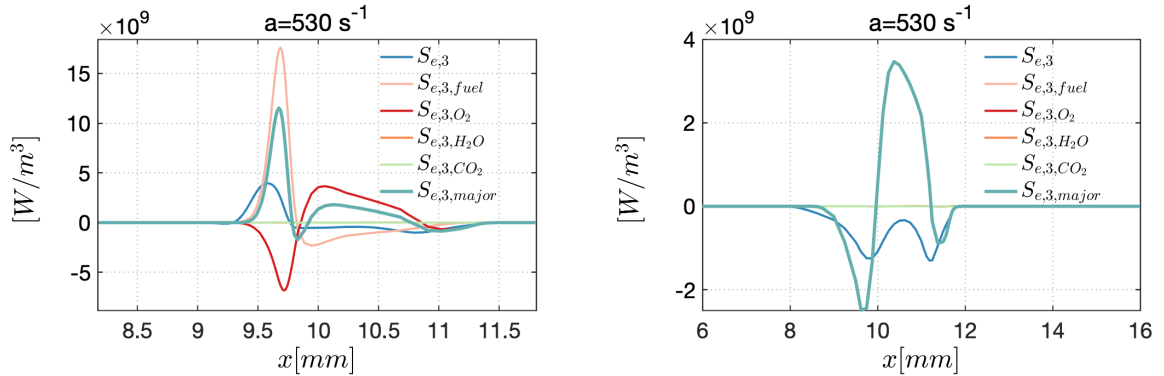


Figure 4: Spatial profiles of  $S_{e,3}$  and  $S_{e,3,major}$ . Left: Methane-oxygen combustion at  $a = 530 s^{-1}$  and  $p = 1$  atm. Right: Hydrogen-oxygen combustion at  $a = 530 s^{-1}$  and  $p = 1$  atm.

### 3.2 Flame-integrated comparison

In order to further investigate the relative contribution of different terms in Eq. (1) to entropy generation, the spatially integrated profiles of the source terms (see Eq. (4)) are examined in this section. Figure 5 shows the flame-integrated results in  $CH_4/O_2$  (left) and  $H_2/O_2$  (right) flames at five different strain rates and  $p = 1$  atm. Figure 5 confirms that for  $CH_4/O_2$ ,  $S_{e,1}$  always plays a leading role in the entropy generation as the strain rate increases, while the contribution of  $S_{e,3}$  is significant with increasing strain

rate. Nevertheless, for  $\text{H}_2/\text{O}_2$  flames, the contribution of  $S_{e,3}$  is comparable to that of  $S_{e,1}$ . Furthermore, Fig. 5 indicates that for both  $\text{CH}_4/\text{O}_2$  and  $\text{H}_2/\text{O}_2$  flames, as the strain rate increases,  $\alpha_1$  decreases significantly and  $\alpha_3$  increases, while  $\alpha_2$  is almost a constant. This suggests that the change in strain rate has a significant impact on entropy generation.

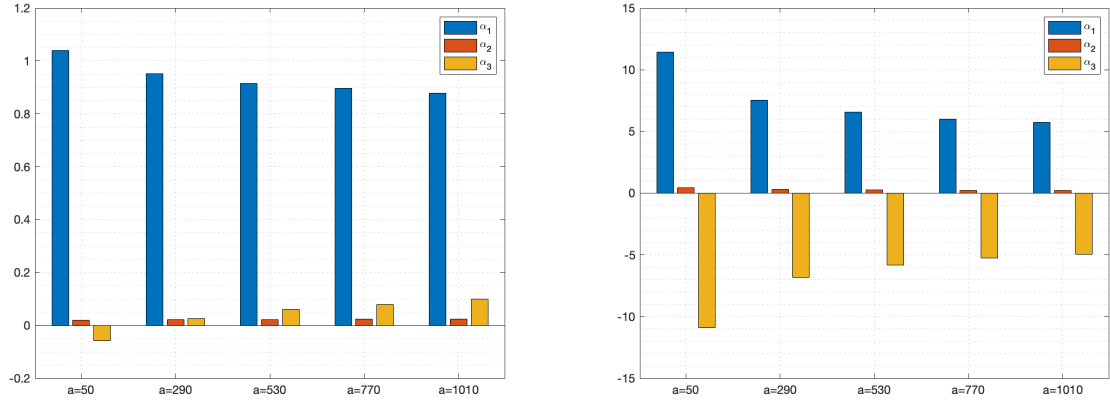


Figure 5: Flame-integrated ratios  $\alpha_1$ ,  $\alpha_2$ , and  $\alpha_3$ . Left:  $\text{CH}_4/\text{O}_2$  flames at five different strain rates and  $p = 1$  atm. Right:  $\text{H}_2/\text{O}_2$  flames at five different strain rates and  $p = 1$  atm.

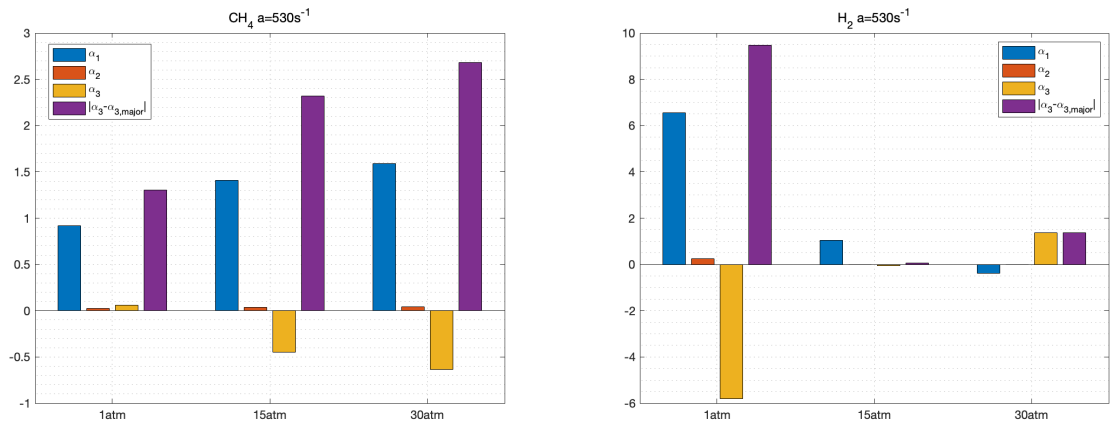


Figure 6: Flame-integrated ratios  $\alpha_1$ ,  $\alpha_2$ ,  $\alpha_3$ , and  $|\alpha_3 - \alpha_{3,major}|$ . Left:  $\text{CH}_4/\text{O}_2$  flames at three different pressures and  $a = 530\text{ s}^{-1}$ . Right:  $\text{H}_2/\text{O}_2$  flames at three different pressures and  $a = 530\text{ s}^{-1}$ .

To investigate the impact of pressure on entropy generation in strained diffusion flames, the change of  $\alpha_1$ ,  $\alpha_2$ , and  $\alpha_3$  with pressure is illustrated in Fig. 6 for both  $\text{CH}_4/\text{O}_2$  and  $\text{H}_2/\text{O}_2$  flames at a fixed strain rate. It is seen that for  $\text{CH}_4/\text{O}_2$  flames,  $\alpha_1$ ,  $\alpha_3$ , and  $|\alpha_3 - \alpha_{3,major}|$  increase significantly with pressure. However, for  $\text{H}_2/\text{O}_2$  flames, the opposite trends are observed. This is due to the fact that the increase in pressure can inhibit dissociation reactions and hence affects entropy generation.

## 4 Conclusion

In this work, the effects of strain rate and pressure on entropy generation are investigated for both CH<sub>4</sub>/O<sub>2</sub> and H<sub>2</sub>/O<sub>2</sub> flames. The results indicate that the contribution of  $S_{e,1}$  and  $S_{e,3}$  are significant for entropy generation. At a fixed pressure, it is seen that the peaks of  $S_e$ ,  $S_{e,1}$ ,  $S_{e,2}$ ,  $S_{e,3}$  obviously increase with the increase in strain rate. Furthermore, the relative contribution of  $S_{e,1}$ ,  $S_{e,2}$  and  $S_{e,3}$  is examined at different strain rates and pressures. It is found that the change in strain rate has a significant impact on entropy generation. Specifically, for both CH<sub>4</sub>/O<sub>2</sub> and H<sub>2</sub>/O<sub>2</sub> flames, as the strain rate increases, the contribution of heat release to entropy generation significantly decreases, while the contribution of reaction-induced species formation is increased. Moreover, it is seen that for CH<sub>4</sub>/O<sub>2</sub> flames, the relative contribution of  $S_{e,1}$ ,  $S_{e,2}$  and  $S_{e,3}$  increases with pressure. However, for H<sub>2</sub>/O<sub>2</sub> flames, the opposite trends are observed. This is because the increase in pressure can inhibit dissociation reactions and hence affects entropy generation. In the future, more calculations will be performed to investigate the impact of strain and pressure on entropy generation.

## References

- [1] F. Marble, S. Candel, Acoustic disturbance from gas non-uniformities convected through a nozzle, *J. Sound Vib.* 55 (2) (1977) 225–243.
- [2] L. Magri, J. O'Brien, M. Ihme, Compositional inhomogeneities as a source of indirect combustion noise, *Journal of Fluid Mechanics* 799 (2016) R4. doi:10.1017/jfm.2016.397.
- [3] K. Nishida, T. Takagi, S. Kinoshita, Analysis of entropy generation and exergy loss during combustion, *Proc. Combust. Inst.* 29 (1) (2002) 869–874, doi:10.1016/S1540-7489(02)80111-0. Proceedings of the Combustion Institute.
- [4] Liu, D., Wang, H., Zhang, Y., Liu, H., Zheng, Z., Yao, M., 2021. On the entropy generation and exergy loss of laminar premixed flame under engine-relevant conditions. *Fuel* 283, 119245. <https://doi.org/10.1016/j.fuel.2020.119245>
- [5] Patki, P., Acharya, V., Lieuwen, T., 2022. Entropy generation mechanisms from exothermic chemical reactions in laminar, premixed flames. *Proc. Combust. Inst.* S1540748922003455. <https://doi.org/10.1016/j.proci.2022.08.069>
- [6] D.G. Goodwin, R.L. Speth, H.K. Moffat, B.W. Weber, Cantera: an object-oriented software toolkit for chemical kinetics, thermodynamics, and transport processes, 2021 Version 2.5.1. 10.5281/zenodo.4527812.
- [7] G. P. Smith, D. M. Golden, M. Frenklach, N. W. Moriarty, B. Eiteneer, M. Goldenberg, C. T. Bowman, R. K. Hanson, S. Song, W. C. Gardiner, V. V. L. Jr., Z. Qin, Gri-mech 3.0.